IEEE Photonics Journal
An IEEE Photonics Society Publication

Optically Tunable Microwave Frequency Downconversion Based on an Optoelectronic Oscillator Employing a Phase-Shifted Fiber Bragg Grating

Volume 10, Number 5, September 2018

Yangxue Ma
Zhiyao Zhang
Jun Yuan
Zhen Zeng
Shangjian Zhang
Yali Zhang
Zhengping Zhang
Dongbing Fu
Jianan Wang
Yong Liu

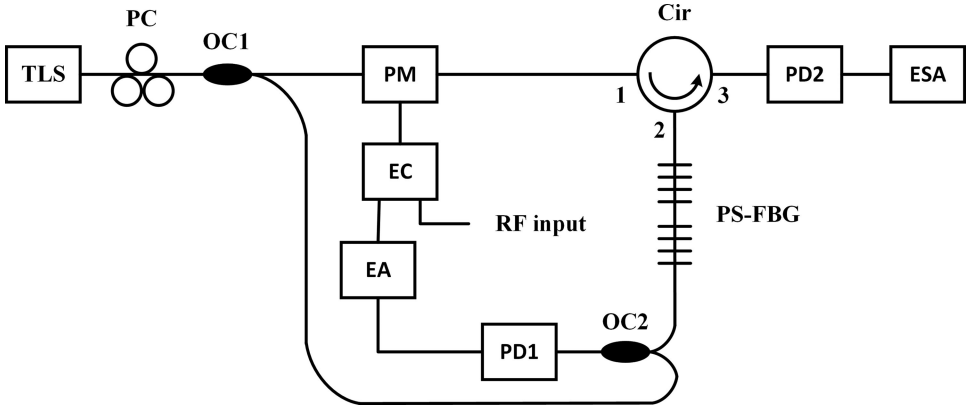

DOI: 10.1109/JPHOT.2018.2867348
1943-0655 © 2018 IEEE

Optically Tunable Microwave Frequency Downconversion Based on an Optoelectronic Oscillator Employing a Phase-Shifted Fiber Bragg Grating

Yangxue Ma,[1] Zhiyao Zhang,[1] Jun Yuan,[2] Zhen Zeng,[1] Shangjian Zhang,[1] Yali Zhang,[1] Zhengping Zhang,[2] Dongbing Fu,[2] Jianan Wang,[2] and Yong Liu[1]

[1]State Key Laboratory of Electronic Thin Films and Integrated Devices, School of Optoelectronic Science and Engineering, University of Electronic Science and Technology of China, Chengdu 610054, China
[2]Science and Technology on Analog Integrated Circuit Laboratory, Chongqing 400060, China

DOI:10.1109/JPHOT.2018.2867348

Manuscript received July 20, 2018; revised August 20, 2018; accepted August 22, 2018. Date of publication September 6, 2018; date of current version September 14, 2018. This work was supported in part by the National Nature Science Foundation of China (Nos. 61575037, 61421002), in part by the Innovation Funds of Collaboration Innovation Center of Electronic Materials and Devices (No. ICEM2015-2001), and in part by the Fundamental Research Funds for Central Universities (ZYGX2015J047). Corresponding authors: Zhiyao Zhang (e-mail: zhangzhiyao@uestc.edu.cn), Jun Yuan (e-mail: yjwlw@semi.ac.cn).

Abstract: We demonstrate an approach to achieve optically tunable microwave frequency downconversion based on an optoelectronic oscillator (OEO) incorporating a tunable microwave photonic filter. The wideband tunable local oscillation (LO) is generated in the OEO through simply tuning the frequency difference between the optical carrier and the reflection notch of a phase-shifted fiber Bragg grating (PS-FBG). The LO and the input radio-frequency (RF) signal are combined and added to the OEO loop by a single-phase modulator. Through transmitting one modulation sideband of the LO via the reflection notch of the PS-FBG and combining it with the optical carrier split from the laser source, the oscillation of the LO in the OEO is maintained. The reflected modulation sidebands of the LO and the RF signal from the PS-FBG are exported out of the OEO loop and enter a narrowband photodetector to achieve optically tunable microwave frequency downconversion. Our method is experimentally evaluated, in which optically tunable LOs in the frequency range 6–15 GHz are generated, and RF signals in the frequency range 7–16 GHz are successfully downconverted to intermediate frequency band around 1 GHz.

Index Terms: Microwave photonics, frequency downconversion, optoelectronic oscillator.

1. Introduction

Microwave frequency downconversion, which converts a radio-frequency (RF) signal to an intermediate frequency (IF) or a baseband signal, is an essential function in RF receivers for various applications such as wireless communication, electronic reconnaissance, and radar. In conventional microwave receivers, electronic mixers are generally employed to achieve frequency downconversion in order to match the input bandwidth of the back-end analog-to-digital converters [1], [2]. The

major drawback of electronic mixers is the limited bandwidth which cannot meet the ever-increasing requirement of wideband applications [3]–[5]. To solve this problem, various photonic-assisted microwave mixers, which are characterized by large bandwidth, immunity to electromagnetic interference, and high isolation between RF and local oscillation (LO) ports, have been proposed and intensively researched in recent years [6]–[28].

The basic frequency downconversion procedure employing a photonic-assisted microwave mixer can be summarized as follows. Firstly, input RF signal is up-converted to the optical domain by an electro-optic modulator. Then, the optically carried microwave signal mixes with an electrical local oscillation (LO) signal at an electro-optic modulator [6]–[17], or with an optical LO signal via nonlinear effect [18]–[20]. Finally, the RF signal and the LO signal in the optical domain beat at a low-speed photo-detector (PD) to obtain an IF signal or a baseband one. The most common photonic-assisted microwave mixer structure leverages two electro-optic modulators in series or in parallel to load the input RF signal and the LO one, respectively [6]–[17]. The prominent advantages of this structure are the high isolation between the RF and LO ports, and the ability to achieve frequency downconversion of an optically carried RF signal at the remote receiver. In the past years, many efforts have been focused on improving the conversion efficiency and the spurious-free dynamic range (SFDR) [8]–[14]. Nevertheless, in order to achieve wideband operation, a broadband tunable electrical LO source is required. The high-frequency electrical LO is generally obtained by multiplying a low-frequency signal through numerous stages of multipliers and amplifiers, which is bulky and cumbersome. Optoelectronic oscillators (OEOs), which have a large operation frequency range, excellent tunability and outstanding phase noise performance [21], [22], are a potential candidate for acquiring a broadband LO, and have been adopted to achieve microwave frequency downconversion in recent years [23]–[28].

In this paper, an optically tunable microwave frequency downconversion scheme based on an OEO employing a phase-shifted fiber Bragg grating (PS-FBG) is proposed. The wideband tunable LO is generated in the OEO loop via a tunable narrowband microwave photonic filter (MPF) which is realized by a PS-FBG and a tunable laser source. The input RF signal is modulated on the optical carrier together with the LO through a single phase modulator in the loop, where the isolation between the RF signal and the OEO-generated LO is realized by detuning the oscillation frequency of the OEO from the frequency of the RF signal. This scheme can achieve wideband optically tunable RF to IF conversion covering multi-tens of GHz frequency range, where the operation bandwidth is determined by the bandwidth of the PS-FBG reflection spectrum, the phase modulator, the PD and the electrical amplifier in the OEO loop. The proposed method is experimentally demonstrated. Optically tunable LOs in the frequency range of 6 GHz to 15 GHz are generated, and RF signals in the frequency range of 7 GHz to 16 GHz are successfully downconverted to IF band around 1 GHz.

2. Operation Principle

The schematic diagram of the proposed OEO-based optically tunable microwave downconverter is shown in Fig. 1. The LO is generated in an OEO loop formed by a tunable laser source (TLS), two optical couplers (OC1 and OC2), a phase modulator, a PS-FBG, a photo-detector (PD1), and an electrical amplifier (EA). Different from the previously proposed OEO-based microwave downconverter schemes which have a fixed LO frequency due to the use of an electrical filter in the loop [23]–[27], this scheme employs a tunable MPF realized by a PS-FBG and a TLS to obtain a wideband tunable LO. Hence, it can achieve tunable microwave frequency downconversion in a broad frequency range. The operation principle of the proposed OEO-based optically tunable microwave downconverter can be described as follows. The continuous-wave (CW) light with a frequency of f_0 from the TLS is split by an optical coupler (OC1) into two paths, with the light wave from the lower path being used as optical carrier, and that from the upper path being modulated by the LO (f_{LO}) together with the input RF signal (f_{RF}) via a phase modulator and an electrical coupler. The modulated light reaches the PS-FBG with a narrow notch in its reflection spectrum, as shown in dashed frame A of Fig. 1. One modulation sideband of the LO ($f_0 + f_{LO}$) falls into the reflection notch and transmits through the PS-FBG. The other modulation sideband of the LO ($f_0 - f_{LO}$) together

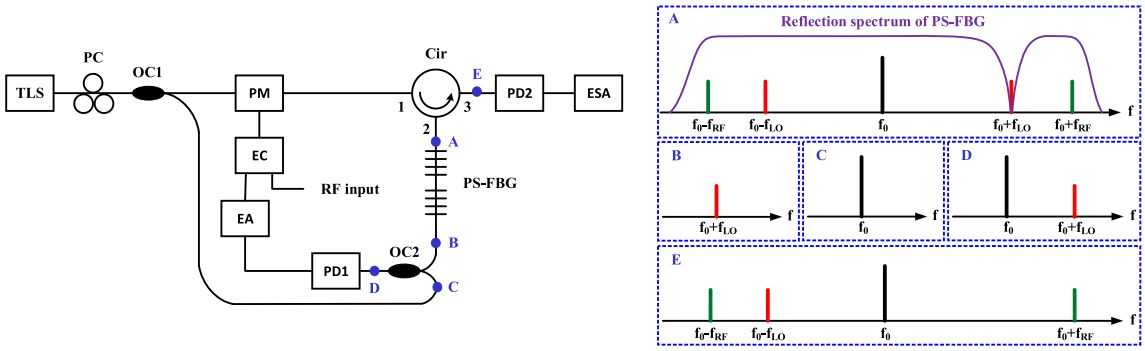

Fig. 1. Schematic diagram of the OEO-based optically tunable microwave downconverter. TLS: tunable laser source; PC: polarization controller; OC: optical coupler; PM: phase modulator; Cir: optical circulator; PS-FBG: phase-shifted fiber Bragg grating; PD: photodetector; EA: electrical amplifier; EC: electrical coupler; ESA: electrical spectrum analyzer.

with the two RF modulation sidebands ($f_0 \pm f_{RF}$) and the optical carrier (f_0) are reflected back to port two of the optical circulator, and output from port three into PD2 for realizing downconversion. In order to maintain the oscillation of the LO signal in the OEO loop, the optical carrier (f_0) which is split from the TLS output is combined with the filtered sideband of the optical microwave LO ($f_0 + f_{LO}$) via OC2, and both of them are photo-detected by PD1 in the OEO loop to recover the electrical LO signal at f_{LO}. The LO originates from noise, whose frequency is determined by the center frequency of the MPF in the loop. In our scheme, the center frequency of the MPF is equal to the frequency difference between the optical carrier and the reflection notch of the PS-FBG. Therefore, through simply tuning the wavelength of the TLS, the LO frequency can be changed once the gain exceeds the loss in the OEO loop. In order to isolate the input RF signal from the LO, the sideband of the RF signal should be kept away from the reflection notch of the PS-FBG to avoid injection locking in the OEO loop, which guarantees that the input RF signal is downconverted to an IF one. In the proposed scheme, this can be easily achieved since the reflection notch bandwidth of a PS-FBG is only tens of MHz.

Mathematically, the optical field at the output of the phase modulator can be written as

$$E_1 = E_0 e^{j\omega_0 t + jm_{LO}\cos(\omega_{LO} t) + jm_{RF}\cos(\omega_{RF} t)} \tag{1}$$

where E_0 is the amplitude of the optical field, and ω_0, ω_{LO} and ω_{RF} are the angular frequencies of the optical carrier, the LO and the input RF signal, respectively. Additionally, $m_{LO} = \pi V_{LO}/V_\pi$ and $m_{RF} = \pi V_{RF}/V_\pi$ are the modulation indexes for the LO and the RF signal, respectively. Thereinto, V_π is the half-wave voltage of the phase modulator, and V_{LO} and V_{RF} are the voltage amplitudes of the LO and the RF signal, respectively. For a small-signal modulation, (1) can be expanded through Jacobi-Anger expansion into

$$\begin{aligned} E_1 \approx\ & E_0 J_0(m_{LO}) J_0(m_{RF}) e^{j\omega_0 t} + jE_0 J_0(m_{RF}) J_1(m_{LO}) e^{j(\omega_0-\omega_{LO})t} + jE_0 J_0(m_{RF}) J_1(m_{LO}) e^{j(\omega_0+\omega_{LO})t} \\ & + jE_0 J_0(m_{LO}) J_1(m_{RF}) e^{j(\omega_0-\omega_{RF})t} + jE_0 J_0(m_{LO}) J_1(m_{RF}) e^{j(\omega_0+\omega_{RF})t} \end{aligned} \tag{2}$$

where $J_n(x)$ is the nth-order Bessel function of the first kind. If the phase-modulated optical field is directly applied to a PD, nothing but a direct current (DC) will be generated since the beating-produced microwave signals which appear in pairs with identical frequency and amplitude but out of phase will cancel out each other completely. In our scheme, one of the modulation sideband of the LO will pass through the PS-FBG (taking $f_0 + f_{LO}$ as an example), Therefore, the balance between the sidebands in the reflected light wave will be broken. After photo-detection in a PD with a large

bandwidth, the output current can be calculated as

$$\begin{aligned} i_{AC} &= R_{PD} E_1 E_1^* \\ &\approx R_{PD} E_0^2 \left\{ J_0^2(m_{LO}) J_0^2(m_{RF}) + J_0^2(m_{RF}) J_1^2(m_{LO}) + 2J_0^2(m_{LO}) J_1^2(m_{RF}) \right. \\ &\quad + 2J_0^2(m_{LO}) J_1^2(m_{RF}) \cos(2\omega_{RF} t) + 2J_0(m_{LO}) J_0^2(m_{RF}) J_1(m_{LO}) \sin(\omega_{LO} t) \\ &\quad + 2J_0(m_{LO}) J_0(m_{RF}) J_1(m_{LO}) J_1(m_{RF}) \cos[(\omega_{RF} + \omega_{LO}) t] \\ &\quad \left. + 2J_0(m_{LO}) J_0(m_{RF}) J_1(m_{LO}) J_1(m_{RF}) \cos[(\omega_{RF} - \omega_{LO}) t] \right\} \end{aligned} \tag{3}$$

where R_{PD} is the responsivity of the PD, and E_0^2 denotes the input optical power of the PD. It can be seen from (3) that, besides DC, frequency components at $2\omega_{RF}$, ω_{LO}, $\omega_{RF} + \omega_{LO}$ and $\omega_{RF} - \omega_{LO}$ are generated. The frequency component of $\omega_{RF} - \omega_{LO}$ represents the downconverted IF signal (i.e., the beat signal between the RF signal and the LO), and can be filtered out by employing a narrowband PD or using an electrical low-pass filter after the PD. In addition, it can be obtained from (3) that the voltage amplitude of the downconverted IF signal can be expressed as

$$V_{IF} = 2RE_0^2 R_{PD} J_0(m_{LO}) J_0(m_{RF}) J_1(m_{LO}) J_1(m_{RF}) \tag{4}$$

where R is the matched resistance which normally equals to 50 Ω. Then, the conversion efficiency of the proposed system can be calculated as

$$G\,(\text{dB}) = P_{IF}\,(\text{dBm}) - P_{RF}\,(\text{dBm}) = 20\log(V_{IF}/V_{RF}) \tag{5}$$

where P_{IF} and P_{RF} are the power of the output IF signal and the input RF signal, respectively.

Furthermore, SFDR can be evaluated when the input is a dual-tone RF signal. In such a case, the optical field at the output of the PM can be written as

$$E_{dual-tone} = E_0 e^{j\omega_0 t + jm_{LO}\cos(\omega_{LO} t) + jm_{RF1}\cos(\omega_{RF1} t) + + jm_{RF2}\cos(\omega_{RF2} t)} \tag{6}$$

where ω_{RF1} and ω_{RF2} are the angular frequencies of the two tones. m_{RF1} and m_{RF2} are the corresponding modulation index. The output voltage after PD can be calculated as

$$V_{dual-tone} = RR_{PD} E_0^2 \left\{ \begin{array}{l} 2J_0^2(m_{RF2}) J_0(m_{LO}) J_0(m_{RF1}) J_1(m_{LO}) J_1(m_{RF1}) \cos[(\omega_{RF1} - \omega_{LO}) t] \\ \quad + 2J_0(m_{LO}) J_0(m_{RF1}) J_0(m_{RF2}) J_1(m_{LO}) J_1(m_{RF2}) J_2(m_{RF1}) \\ \quad \times \cos[(2\omega_{RF1} - \omega_{RF2} - \omega_{LO}) t] + \cdots \end{array} \right\} \tag{7}$$

where the voltage amplitudes of the IF signal ($\omega_{RF1} - \omega_{LO}$) and the 3rd-order intermodulation distortion (IMD3) ($2\omega_{RF1} - \omega_{RF2} - \omega_{LO}$) are obtained. Then the corresponding power of the downconverted IF signal and IMD3 distortion, which are denoted as P_{RF1-LO} and $P_{2RF1-RF2-LO}$, can be calculated. Finally, the SFDR of the system can be calculated as

$$SFDR\left(\text{dB}\cdot\text{Hz}^{2/3}\right) = P_{RF1-LO}\,(\text{dBm}) - \frac{1}{3}P_{2RF1-RF2-LO}\,(\text{dBm}) - \frac{2}{3}NF\,(\text{dBm/Hz}) \tag{8}$$

where NF is the normalized noise floor of the downconversion system.

3. Experimental Results and Discussion

An experiment based on the configuration shown in Fig. 1 is performed. The CW optical carrier is generated by a TLS (Anritsu MG9638A) which has a wavelength tuning range from 1500 nm to 1580 nm and a tuning step of 1 pm. A 10 GHz electro-optic phase modulator (JDSU PM-150-080) combined with an electrical coupler (HP 87304C, 2–26.5 GHz) are employed to modulate the LO and the input RF signal onto the light wave. The reflection spectrum of the PS-FBG (TeraXion) utilized in the OEO is from 1544.29 nm to 1545.22 nm, which has a notch located at 1544.89 nm. Two cascaded electrical amplifiers are used to compensate the loss in the OEO loop, where the first one (Narda 60583) is with an operation frequency range from 6 GHz to 18 GHz and a small-signal gain of 45 dB, and the second one (Multilink MTC5515) is with an effective operation frequency

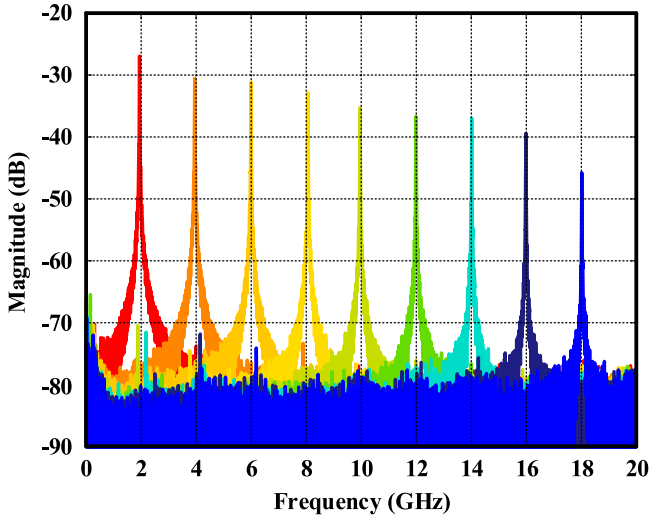

Fig. 2. Superimposed frequency response of the MPF employed in the OEO with a tuning step of 2 GHz.

range from DC to 20 GHz and a small-signal gain of 23 dB at the low-frequency stage. Additionally, two PDs (New Focus, Model 1414) with a 3 dB bandwidth of 25 GHz, a responsivity of 0.7 A/W, and a maximum conversion gain of 17 V/W are incorporated in the loop and out of it to recover the LO and to achieve microwave frequency downconversion, respectively. An electrical spectrum analyzer (ESA, Agilent E4448A) is adopted to measure the generated LO and the downconverted IF signal.

Firstly, the frequency response of the tunable MPF in the OEO loop is measured by using a vector network analyzer (VNA, Keysight N5224A). During the measurement, the OEO loop is opened, and only one electrical amplifier (Multilink MTC5515) is connected to PD1. Through setting the wavelength of the optical carrier in the reflection spectrum of the PS-FBG and tuning it in a fine step of 1 pm, the center frequency of MPF is changed with a step of about 125 MHz. Fig. 2 shows the superimposed frequency responses of the MPF covering a frequency range of DC to 20 GHz with a frequency tuning step of 2 GHz, in which the 3 dB bandwidth of the MPF is about 10 MHz. The decreasing response at the high-frequency stage is due to the degraded response of the phase modulator, the PD and the electrical amplifier employed in the experimental setup. It should be pointed out that this frequency range can be further increased by employing a PS-FBG with a wider reflection spectrum, and using a phase modulator, a PD and an electrical amplifier with a broader bandwidth. Through inserting the other electrical amplifier (Narda 60583) and the electrical coupler into the link, the link gain of the open loop is measured. Fig. 3 presents the superimposed frequency responses of the open loop with a frequency tuning step of 1 GHz. It can be seen from Fig. 3 that, constrained by the bandwidth of the electrical amplifier (Narda 60583), the link gain of the open loop exceeds 0 dB only in the frequency range of 6 GHz to 17 GHz, which puts an ultimate limit to the operation bandwidth of the OEO in the experiment.

Then, the OEO loop is closed, but with the electrical coupler connected in the reverse direction, where one output port of the electrical coupler is connected to the ESA to measure the generated LO. Fig. 4 shows the superimposed spectra of the generated LOs in the frequency range of 6 GHz to 15 GHz with a coarse tuning step of 1 GHz. Through finely tuning the TLS, LOs in the frequency range of 5.8 GHz to 15.5 GHz can be generated in our experiment. Additionally, it needs to be noted that the 2nd-order harmonic of the LO is also generated by the OEO loop, which can be explained as follows. Firstly, 2nd-order harmonic of LO is generated by the phase modulator because of its nonlinearity characteristics. Then, the 2nd-order harmonic is suppressed by the MPF whose out-of-band rejection ratio is about 46 dB at 6 GHz as shown in Fig. 2. Finally, the 2nd-order harmonic is enhanced after the EA due to the nonlinear response of the EA. Therefore, the power of the

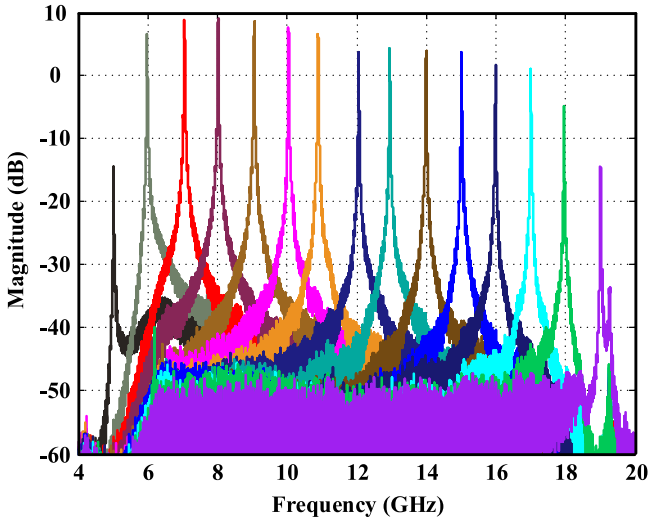

Fig. 3. Superimposed frequency response of the open loop with a tuning step of 1 GHz.

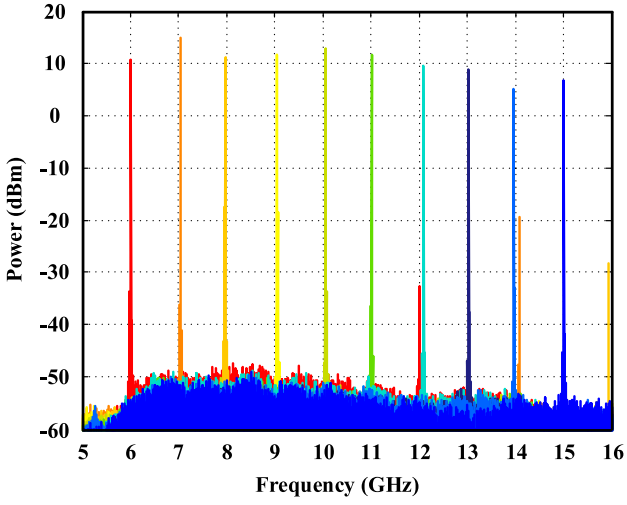

Fig. 4. Superimposed spectra of the generated LOs ranging from 6 GHz to 15 GHz with a tuning step of 1 GHz.

2nd-order harmonic, which is evaluated by the 2nd-order harmonic distortion ratio of this OEO loop, is mainly determined by the out-of-band rejection ratio of the MPF, the nonlinearity of the EAs and the bandwidth of the PD. A 2nd-order harmonic distortion ratio over 35 dB is realized in the experiment as shown in Fig. 4.

Whereafter, the electrical coupler is connected as shown in Fig. 1 to test the downconversion performance. The RF signal generated by a signal generator (Agilent E8254A) is combined with the LO to modulate the light wave via the phase modulator. Fig. 5(a)–(d) give the measured electrical spectra at the output of PD2 when the input RF signals are with frequencies of 7 GHz, 10 GHz, 13 GHz and 16 GHz, respectively, where the LO frequencies are finely tuned to 6 GHz, 9 GHz, 12 GHz and 15 GHz, correspondingly. It can be seen from Fig. 5 that the RF signals are successfully downconverted to IF band around 1 GHz. The residual RF signals in the output are due to the unbalanced modulation sidebands in the reflected light wave.

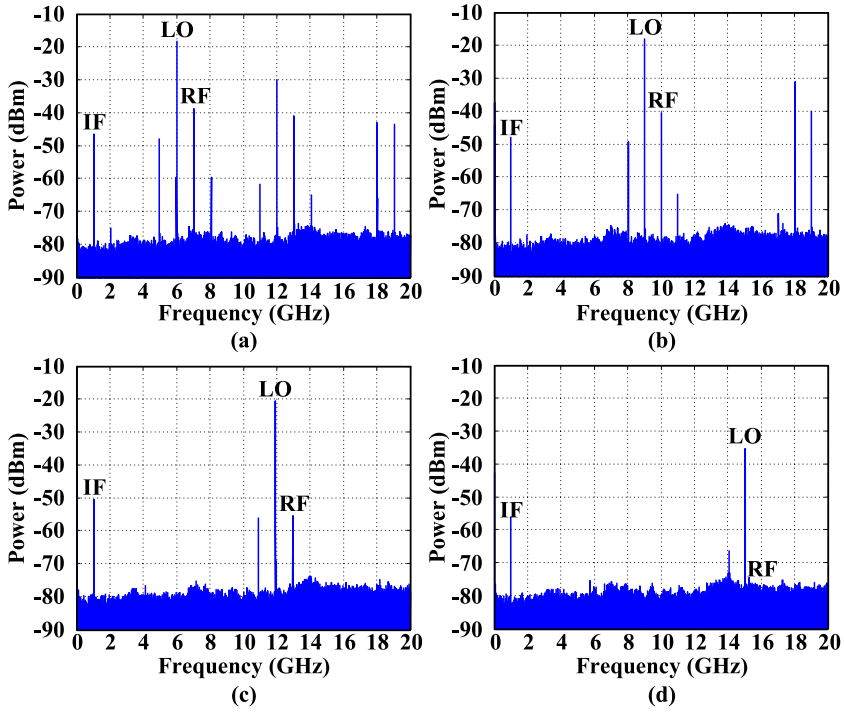

Fig. 5. Measured electrical spectra at the output of PD2 (RBW = 100 kHz). (a) RF: 7 GHz, LO: 6 GHz. (b) RF: 10 GHz, LO: 9 GHz. (c) RF: 13 GHz, LO: 12 GHz. (b) RF: 16 GHz, LO: 15 GHz.

Then, the conversion efficiency is assessed. In the experiment, the power of the LO injected into the PM is measured to be 13 dBm (i.e., peak voltage of 1.4V) at 9 GHz as shown in Fig. 4. Additionally, the power of the input RF signal is set to 10 dBm (i.e., peak voltage of 1V) at 10 GHz, and the half-wave voltage of the PM is about 11.3 V@10 GHz. The optical power injected into PD2 is measured to be about −0.5 dBm. Since the maximum input optical power cannot exceed 3 dBm due to the power handling capacity of PD2, we do not employ an optical amplifier to increase the optical power injected into PD2. Through substituting the experimental parameters into (5), the theoretical conversion efficiency at 10 GHz is calculated to be −56.2 dB. Meanwhile, Fig. 6 shows the measured conversion efficiency versus input RF frequency when the frequency of the IF signal is set to be 1 GHz and the LO is tuned to be a lowside one. As can be seen from Fig. 6, the conversion gain at 10 GHz is measured to be −56.6 dB in the experiment, which agrees well with the theoretical result of −56.2 dB. The relatively low conversion efficiency is mainly due to the low optical power injected into PD2. Hence, a higher conversion efficiency can be obtained by employing a high-power laser source (or using optical amplifier) and a PD with a higher saturation input optical power, or simply cascading an electrical amplifier after the PD. Besides, substitution of the PM with a Mach-Zehnder modulator (MZM) biased at its minimum transmission point (i.e., realizing suppressed-carrier dual-sideband modulation) can also help to enhance the conversion efficiency, since the optical carrier has the highest power in the optical signal, but has nothing to do with the downconversion (the IF signal is acquired by the beating between the 1st-oder modulation sidebands of the RF signals and the LO). Therefore, carrier suppression is favorable for fully utilizing the power handling capacity of the PD to achieve downconversion. In addition, the dowconverted IF signal can be filtered out through using a narrow PD or cascading a low-pass filter after the PD.

Finally, the SFDR of the downconverter is tested by applying two RF tones centered at 9.000 GHz and 9.010 GHz with identical power, in which the frequency of the LO is tuned to be 7.973 GHz. Fig. 7 exhibits the downconverted two IF tones centered at 1.032 GHz, where the resolution bandwidth (RBW) of the ESA is set to be 510 kHz. Based on the measured result, the noise floor of the

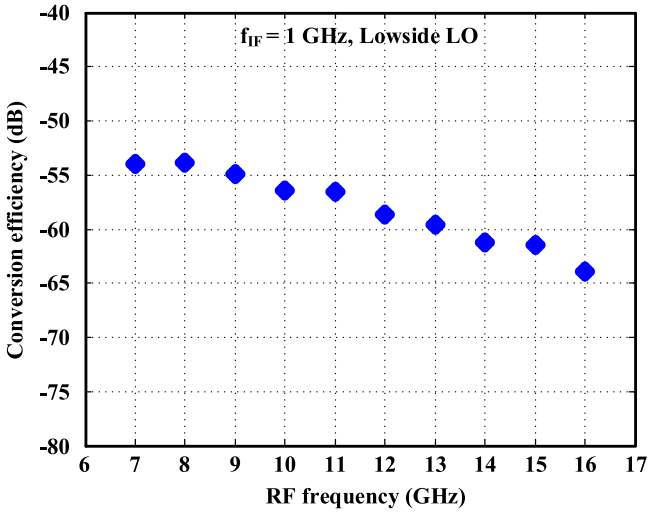

Fig. 6. Measured conversion efficiency versus input RF frequency when the IF frequency is set to be 1 GHz and the LO is tuned to be a lowside one.

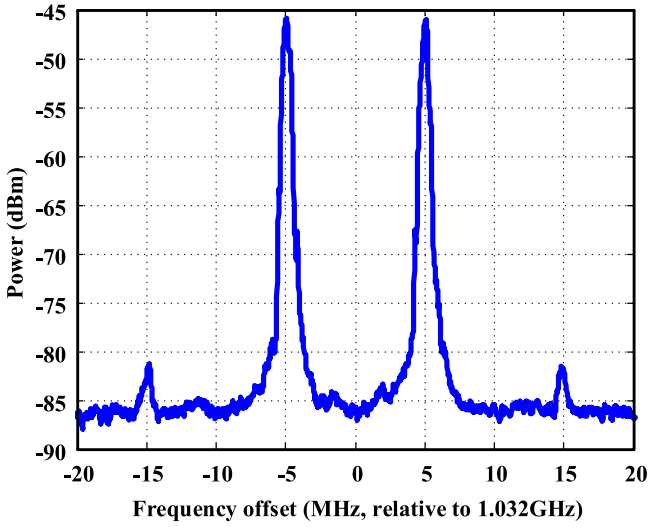

Fig. 7. Measured spectrum of the downconverted IF signal when two RF tones centered at 9.000 GHz and 9.010 GHz with identical power are injected into the downconverter (RBW = 510 kHz).

downconverter is calculated to be −145 dBm/Hz. Fig. 8 presents the measured output power of the fundamental tone and the IMD3 tone under various input RF power, together with the noise floor, which indicates that the SFDR of the downconverter is 74.9 dB·$Hz^{2/3}$. Similar to the conversion efficiency, the SFDR can be calculated by substituting the parameters of the devices into (8). The theoretical SFDR of the system is calculated to be 79.0 dB·$Hz^{2/3}$, which is 4 dB higher that the experimental result. The small mismatch between the experimental and theoretical results might be induced by the truncation error of the Jacobi-Anger expansion in the equation, or the interpolation error of the signal and the 3rd-order distortion in Fig. 8. Moreover, it can be seen from (8) that the SFDR of the proposed system is proportional to the difference between the output 3rd-order intercept point (OIP3) and the noise floor. The noise floor (−145 dBm/Hz) in the experiment is mainly limited by the background noise of PD2, which is hard to decrease significantly. Hence, the primary method to enhance the SFDR of the system is to enhance the OIP3, i.e., improve the power of the IF signal

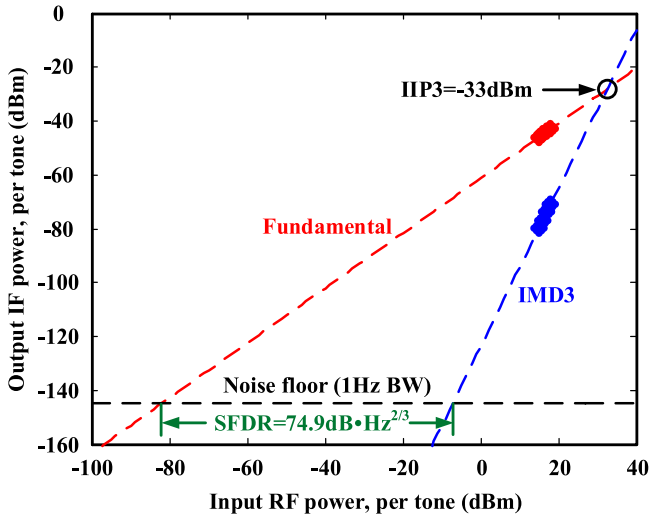

Fig. 8. Measured SFDR of the downconverter.

after PD2 while the input RF power and the noise floor are maintained. This can be achieved by employing a high-power laser source (or using optical amplifier) and a PD with a higher saturation input optical power, or replacing the PM with an MZM biased at its minimum transmission point.

It should also be pointed out that the 2nd-order harmonic of the LO will have a certain impact on the system performance. When the input is a single-tone RF signal (e.g., 9 GHz), normally, the frequency of the LO should be turned to be a little lower than the RF frequency (e.g., 8 GHz) to obtain an IF signal (e.g., 1 GHz). However, due to the existence of the 2nd-order harmonic of the LO, when the LO frequency is turned to be half of the normal one (i.e., 4 GHz), an IF signal with a frequency of 1 GHz can also be obtained. This unexpected downconversion is induced by the beating between the modulation sideband of the RF signal and that of the 2nd-order LO harmonic, whose conversion efficiency is very low since the 2nd-order harmonic suppression ratio of the OEO is over 35 dB in the experiment. In addition, when the input is a multi-tone RF signal with frequencies covering multiple octaves (e.g., 9 GHz and 17 GHz), the frequency of the LO should normally be set as 8 GHz to downconvert the 9 GHz RF signal to an IF signal with a frequency of 1 GHz. Nevertheless, because of the existence of the 2nd-order harmonic of the LO, the 17 GHz RF signal will also be downconverted to an unexpected IF signal with a frequency of 1 GHz, which will mix with the IF signal downconverted from 9 GHz RF signal. In the experiment, this interference is not remarkable since the 2nd-order harmonic suppression ratio of the OEO is greater than 35 dB. Further optimization of the gain in the OEO loop can enhance the 2nd-order harmonic suppression ratio, which is favorable for reducing this interference in the multiple octave operation.

Furthermore, PS-FBGs play a critical role in the proposed microwave frequency downconversion scheme. On one hand, the reflection notch of the PS-FBG is utilized to select out one modulation sideband of the LO and transmit it through the OEO loop to maintain the oscillation of the LO by combining it with the optical carrier split from the laser source. On the other hand, the reflection spectrum of the PS-FBG is used to extract the RF modulation sidebands and the residual LO modulation sideband out of the OEO loop to achieve downconversion, and more importantly to avoid RF signal oscillation in the loop. In general, the reflection notch is located near the center of the reflection spectrum of a PS-FBG. Based on the principle shown in Fig. 1, it can be easily seen that the operation bandwidth of the proposed downconverter is almost a quarter of the reflection bandwidth of the PS-FBG. In our experimental setup, the reflection bandwidth of the PS-FBG is about 0.97 nm, which indicates the tunable frequency range of the OEO can reach nearly 30 GHz. The restricted LO frequency tuning range from 6 GHz to 15 GHz actually achieved is due to the limited bandwidth of the phase modulator, the PD1 and the electrical amplifiers employed

in the experiment. In addition, the reflection bandwidth of the PS-FBG can be increased to a few nanometers through enhancing the amplitude of the induced reflection index perturbation in the fiber grating writing process [29]. Hence, the proposed optically tunable microwave frequency downconversion has the potential to cover an operation bandwidth of multi-tens of GHz.

4. Conclusion

We demonstrate an optically tunable microwave frequency downconverter based on an OEO incorporating a tunable MPF realized by a PS-FBG and a TLS. The LO frequency is equal to the frequency difference between the optical carrier and the reflection notch of the PS-FBG, which can be freely varied through tuning the wavelength of the TLS. The proposed method was experimentally evaluated, in which optically tunable LOs in the frequency range of 6 GHz to 15 GHz were generated, and RF signals in the frequency range of 7 GHz to 16 GHz were successfully downconverted to IF band around 1 GHz. The operating frequency range can be extended by employing wideband devices including a PS-FBG, a phase modulator, a PD and an electrical amplifier. Additionally, the SFDR can be further improved by employing PD2 with a higher saturation input power, or replacing the PM with an MZM biased at its minimum transmission point.

References

[1] O. Jamin, "RF receiver architecture state of the art," in *Broadband Direct RF Digitization Receivers*. Cham, Switzerland, Springer, 2014, pp. 1–6.
[2] J. Lasker, B. Matinpour, and S. Chakraborty, "Review of receiver architectures," in *Modern Receiver Front-Ends: Systems, Circuits, and Integration*. New York, NY, USA: Willey, 2004, pp. 28–32.
[3] M. E. Manka, "Microwave photonics electronic warfare technologies for Australian defence," in *Proc. IEEE Int. Top. Meet. Microw. Photon.*, 2008, pp. 1–2.
[4] R. W. Ridgway, C. L. Dohrman, and J. A. Conway, "Microwave photonics programs at DARPA," *J. Lightw. Technol.*, vol. 32, no. 20, pp. 3428–3439, Oct. 2014.
[5] T. R. Clark and R. Waterhouse, "Photonics for RF front ends," *IEEE Microw. Mag.*, vol. 12, no. 3, pp. 87–95, May 2011.
[6] G. K. Gopalakrishnan, W. K. Burns, and C. H. Bulmer, "Microwave-optical mixing in $LiNbO_3$ modulators," *IEEE Trans. Microw. Theory Techn.*, vol. 41, no. 12, pp. 2383–2391, Dec. 1993.
[7] A. C. Lindsay, G. A. Knight, and S. T. Winnall, "Photonic mixers for wide bandwidth RF receiver applications," *IEEE Trans. Microwave Theory Techn.*, vol. 43, no. 9, pp. 2311–2317, Sep. 1995.
[8] R. Helkey, J. C. Twichell, and C. Cox, "A down-conversion optical link with RF gain," *J. Lightw. Technol.*, vol. 15, no. 6, pp. 956–961, Jun. 1997.
[9] A. Karim and J. Devenport, "High dynamic range microwave photonic links for RF signal transport and RF-IF conversion," *J. Lightw. Technol.*, vol. 26, no. 15, pp. 2718–2724, Aug. 2008.
[10] V. R. Pagán, B. M. Haas, and T. E. Murphy, "Linearized electrooptic microwave downconversion using phase modulation and optical filtering," *Opt. Exp.*, vol. 19, no. 2, pp. 883–895, Jan. 2011.
[11] E. H. W. Chan and R. A. Minasian, "Microwave photonic downconverter with high conversion efficiency," *J. Lightw. Technol.*, vol. 30, no. 23, pp. 3580–3585, Dec. 2012.
[12] Y. S. Gao *et al.*, "An efficient photonic mixer with frequency doubling based on a dual-parallel MZM," *Opt. Commun.*, vol. 321, pp. 11–15, Jun. 2014.
[13] P. X. Li, W. Pan, X. H. Zou, S. L. Pan, B. Luo, and L. S. Yan, "High-efficiency photonic microwave downconversion with full-frequency-range coverage," *IEEE Photon. J.*, vol. 7, no. 4, Aug. 2015, Art. no. 5500907.
[14] L. Huang *et al.*, "Photonic downconversion of RF signals with improved conversion efficiency and SFDR," *IEEE Photon. Technol. Lett.*, vol. 28, no. 8, pp. 880–883, Apr. 2016.
[15] Z. Z. Tang and S. L. Pan, "A reconfigurable photonic microwave mixer using a 90° optical hybrid," *IEEE Trans. Microw. Theory Techn.*, vol. 64, no. 9, pp. 3017–3025, Sep. 2016.
[16] J. X. Liao, X. P. Zheng, S. Y. Li, H. Y. Zhang, and B. K. Zhou, "High-efficiency microwave photonic harmonic downconversion with tunable and reconfigurable filtering," *Opt. Lett.*, vol. 39, no. 23, pp. 6565–6568, Dec. 2014.
[17] X. Fang, M. Bai, X. Z. Ye, J. G. Miao, and Z. Zheng, "Ultra-broadband microwave frequency down-conversion based on optical frequency comb," *Opt. Exp.*, vol. 23, no. 13, pp. 17111–17119, Jun. 2015.
[18] C. Bohémond, T. Rampone, and A. Sharaiha, "Performance of a photonic microwave mixer based on cross-gain modulation in a semiconductor optical amplifier," *J. Lightw. Technol.*, vol. 29, no. 16, pp. 2402–2409, Aug. 2011.
[19] H. J. Kim and J. I. Song, "All-optical frequency downconversion technique utilizing a four-wave mixing effect in a single semiconductor optical amplifier for wavelength division multiplexing radio-over-fiber applications," *Opt. Exp.*, vol. 20, no. 7, pp. 8047–8054, Mar. 2012.
[20] H. Huang, X. Wu, J. Wang, J. Y. Yang, A. Voskoboinik, and A. E. Willner, "Nondegenerate four-wave-mixing-based radio frequency up/downconversion using parametric loop mirror," *Opt. Lett.*, vol. 36, no. 23, pp. 4593–4595, Dec. 2011.
[21] L. Maleki, "Sources: The optoelectronic oscillator," *Nature Photon.*, vol. 5, no. 12, pp. 728–730, Dec. 2011.

[22] X. H. Zou *et al.*, "Optoelectronic oscillarors (OEOs) to sensing, measurement, and detection," *IEEE J. Quantum. Electron.*, vol. 52, no. 1, Jan. 2016, Art. no. 0601116.
[23] W. Shieh, S. X. Yao, G. Lutes, and L. Maleki, "Microwave signal mixing by using a fiber-based optoelectronic oscillator for wavelength division multiplexed systems," in *Proc. Opt. Fiber Commun. Conf. Tech. Dig.*, Dallas, TX, USA, 1997, pp. 358–359.
[24] D. Zhu, S. L. Pan, S. H. Cai, and D. Ben, "High-performance photonic microwave downconverter based on a frequency-doubling optoelectronic oscillator," *J. Lightw. Technol.*, vol. 30, no. 18, pp. 3036–30425, Sep. 2012.
[25] T. Sun *et al.*, "Microwave photonic down-conversion based on a wideband tunable optoelectronic oscillator," presented at the Asia Commun. Photon. Conf., Beijing, China, 2013, Paper AF2F.3.
[26] Z. Z. Tang, F. Z. Zhang, and S. L. Pan, "Photonic microwave downconverter based on an optoelectronic oscillator using a single dual-drive Mach-Zehnder modulator," *Opt. Exp.*, vol. 22, no. 1, pp. 305–310, Jun. 2014.
[27] J. Y. Lee and J. I. Song, "Photonic frequency down-converter based on a frequency-doubling OEO using two cascaded EAMs," *IEEE Photon. Technol. Lett.*, vol. 29, no. 18, pp. 1529–1531, Sep. 2017.
[28] H. C. Yu *et al.*, "Simple photonic-assisted radio frequency down-converter based on optoelectronic oscillator," *Photon. Res.*, vol. 2, no. 4, pp. B1–B4, Aug. 2014.
[29] T. Erdogan, "Fiber grating spectra," *J. Lightw. Technol.*, vol. 15, no. 8, pp. 1277–1294, Aug. 1997.